AVALANCHERS: Detection Device For Finding People After An Avalanche

David Chavez, Angel Vega, Antonio Baca, and Raul A. Villalobos

Supercomputing, Capital High School

Irina Cislaru, Barbara Teterycz, and Dave Ritter

April 10, 2026

Contents

Abstract

Every year, around 150 lives are taken by avalanches worldwide. (National Weather Service, n.d.). Two causes contribute towards this high count: Improper examination of the snow (NOAA, n.d.), which could misguide traveller(s) into clustering up in an unsafe area, and ineffective methods for locating lost individuals (Bridgeport Avalanche Center, n.d.), which could make the difference between life and death for an individual. This project explores the idea of locating individuals after a snowpack falls on them, in turn, creating a device that could detect individuals under snow. This device was built using affordable – but effective components, with the ultimate goal of saving the lives of skiers and townsfolk who can unknowingly fall under an avalanche.

Literature review

Annually, avalanches have taken around 150 lives according to the National Weather Service, with some of the deadliest avalanches being the 1970 Huascarán avalanche in Peru, with a death toll of ~30,000 people, 1916's "White Friday" in Italy with a death toll of 2,000-10,000 people, and the 1962 Huascarán avalanche with a death toll of ~4000 people. It is important to grasp the true size of these numbers and understand what affected the ability to save many of these lives.

Furthermore, many avalanche deaths were caused by individuals being lost underneath the snow, with Scott et al. stating that "The majority of avalanche victims (...) died as a result of asphyxiation" and "Most avalanche victims remain alive directly after burial and have the potential for a successful live recovery." (Scott et al., 2007).

Throughout our research, we found that many ski areas use a system called RECCO. According to Grassegger et al., “The RECCO Rescue System (...) is considered standard rescue equipment in some areas together with transceivers, a probing team, and avalanche dogs.” (Grassegger et al, 2016). However, RECCO has been criticized for interference issues, which Genswein et al. describe as “The transceiver shows arbitrary distance and direction indications exclusively caused by interference in an area where there is no buried subject or the distance to the buried subject is much greater than the maximum range of the receiver.” (Genswein et al., n.d.). The fundamental issue with RECCO is the apparent size of the transceiver, which can become easily blocked or interfered with.

In contrast, we found that Yagi-Uda antennas, in particular, are beneficial for large-scale directional sweeps, which can cover a wider area and receive less interference from smaller objects. These antennas are “widely used as a directional antenna on the HF, VHF and UHF bands.” (Wikimedia Foundation, n.d.). This makes it very appealing for interference analysis, as its relatively low cost and ease-of-use can make it versatile in multiple use cases.

Methodology

The idea for this project first began when our team had a conversation about skiing; the primary concern of most of our team was the chance of an avalanche occurring. This conversation brought up the idea of creating a device that could potentially save people’s lives. We proposed the use of ground-penetrating radar, or GPR for short, which uses radio waves to detect objects underground. We first had to find what type of antenna would be compatible with GPR and its appropriate frequency range.

Initial Inquiry

Initially, we began with a log-periodic antenna, which is a directional broadband antenna, but it had insufficient directionality and gain, which would cause issues when analyzing data collected from the analysis device. Doing further research, we found that Yagi-Uda antennas were the most suitable for our project. Their cost-effectiveness, directionality, and increased gain would cause fewer issues throughout the development process and analysis of data.

Antenna construction

The construction of a Yagi-Uda antenna was done using a dedicated calculator, which allowed the antennas to be fine-tuned to work with our project's frequency range of 885MHz, which is ideal for penetrating snow and debris at a decent resolution. The goal of this antenna was to broadcast and detect changes in its received signal. Due to object attenuation causing gain loss, we used two amplifiers with a +50dB gain, which added enough gain for the system to detect individuals.

Figure I: Yagi antenna diagram

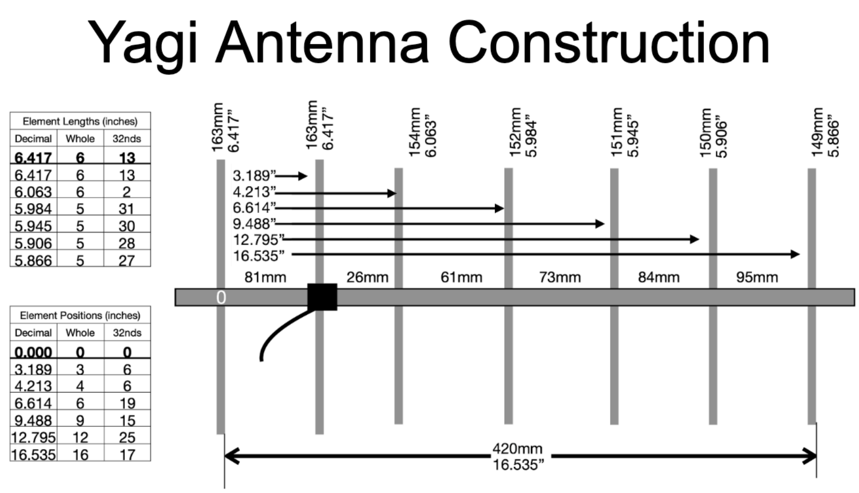

Element Lengths (inches)		
Decimal	Whole	32nds
6.417	**6**	**13**
6.417	6	13
6.063	6	2
5.984	5	31
5.945	5	30
5.906	5	28
5.866	5	27

Element Positions (inches)		
Decimal	Whole	32nds
0.000	**0**	**0**
3.189	3	6
4.213	4	6
6.614	6	19
9.488	9	15
12.795	12	25
16.535	16	17

This diagram describes the exact measurements needed to construct the project's Yagi-Uda antenna.

For testing the functionality of this Yagi-Uda antenna, we used our log-periodic antenna, which would send out signals in the 885MHz range, along with a vector network analyzer, or VNA for short, and measured the amount of signal that was being received by the Yagi-Uda antenna in multiple directions. The Yagi-Uda antenna was deemed sufficiently effective at measuring signals unidirectionally, as it had a gain of +10dB, and a front-to-back ratio of 25dB in comparison to the log-periodic, which only had +5dB and 15dB respectively.

Figure II: Yagi-Uda antenna prototype

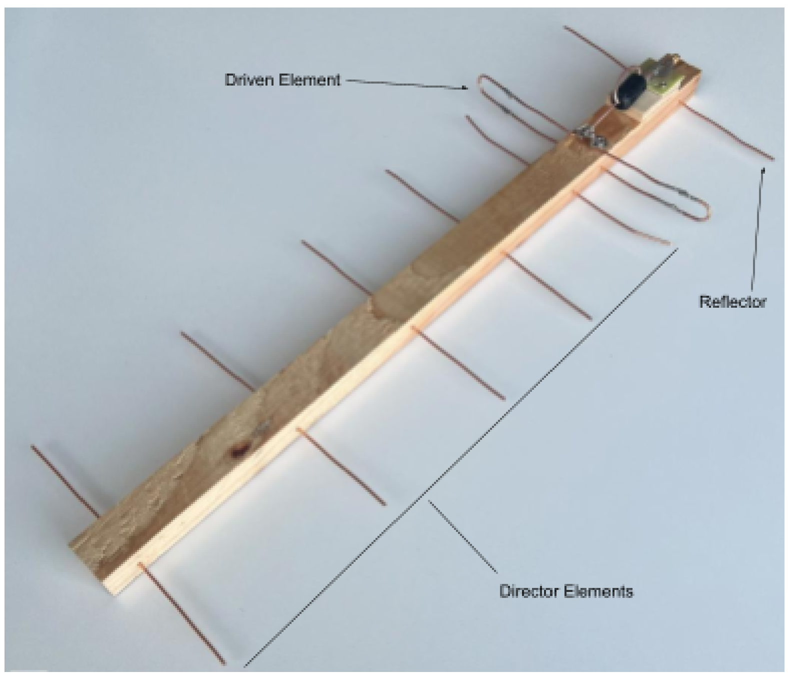

This figure shows the first Yagi-Uda prototype with labelled elements.

Prototype

Our prototype consisted of a woodstock base, copper wire, and a balun (balanced-to-unbalanced) converter. Yagi-Uda antennas work by connecting a signal from the balun of the system to the driven element of the antenna. From here, the signal travels down the director elements in sinusoidal and cosinusoidal forms. The reflector on the back acts as a blocking element for the reverse signal.

Figure III: Yagi-Uda antenna function (Wikimedia Foundation et al., n.d.)

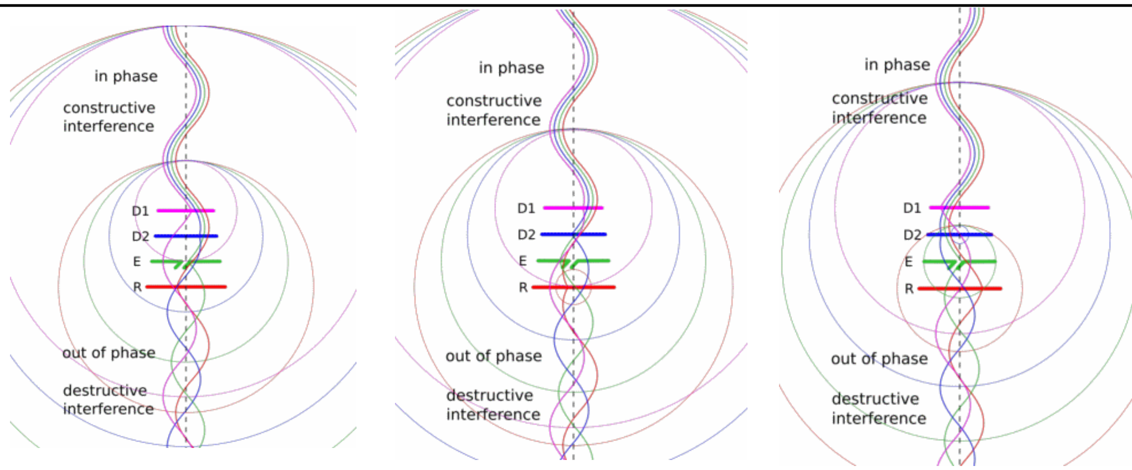

This figure demonstrates how a Yagi-Uda antenna functions.

Our final antenna had a wavelength of ~0.339m, with a supporting structure length of 0.407m and 7 antenna elements, with spacing between those elements varying from 26mm to 95mm. The antenna as well had a Main Lobe angle width of ~45-60deg in the magnetic (near) field, and 35-45deg in the electromagnetic (far) field.

Vector network analyzer system

The construction of the complete system consisted of a vector network analyzer, in which a signal sent from it moves through the first amplifier (+20dB) and through the second amplifier (+30dB) leading the signal to gain +50dB. This signal would then travel through the transmitting antenna and reflect off of a person under snow and come back to the receiving end of the system. This received signal would then be sent to a computer in which a python script would analyze the sweep and tell us if there was a significant change in signal indicating a person was underneath the snow.

Figure IV: System Diagram
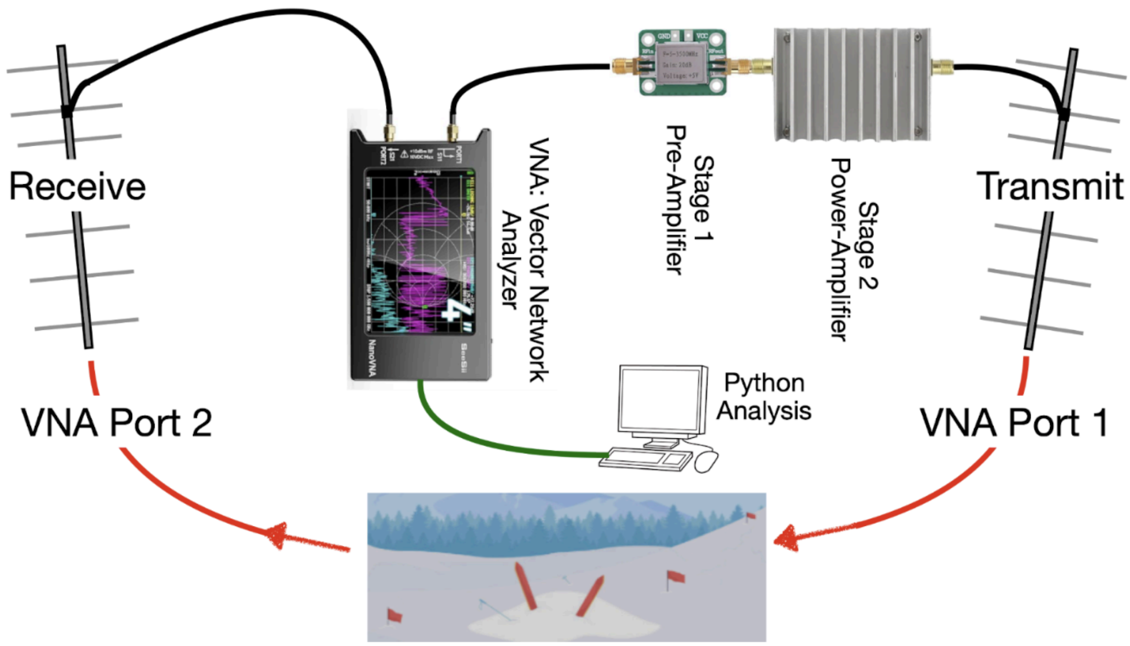
This figure represents a simplified diagram of our system.

Figure V: Angular Geometry of Antennas

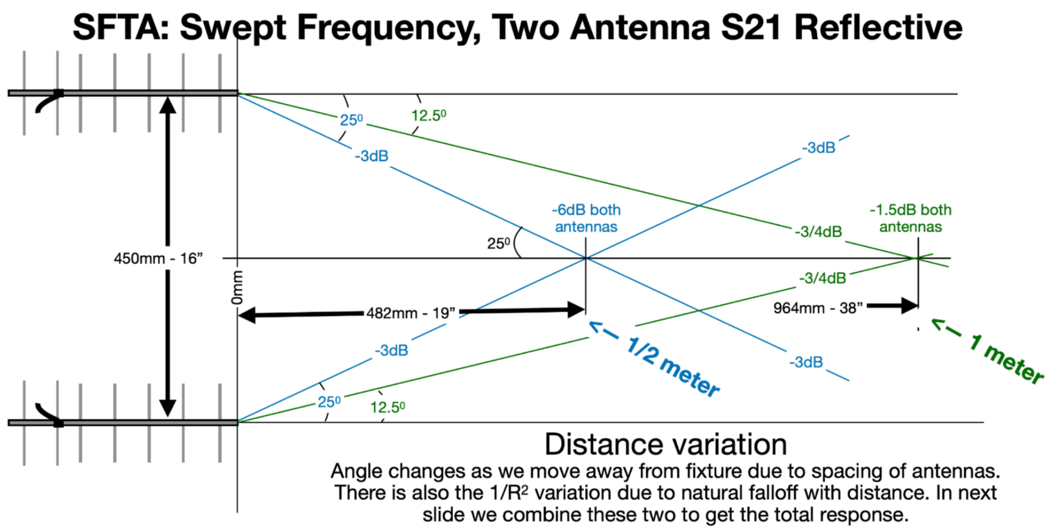

This figure demonstrates the angular geometry of the return of a sweep function.

Throughout our testing, we saw that the above figure accurately depicts how distance can impact the strength of the signal. Our results are similar to an inverse representation of the inverse square law, which states that the further you are from a wave source, the more signal loss you are expected to have. (Talbot-Smith, 1993). The figure below demonstrates what we had encountered with our testing.

Figure VI: Inverse Square Law vs. Testing
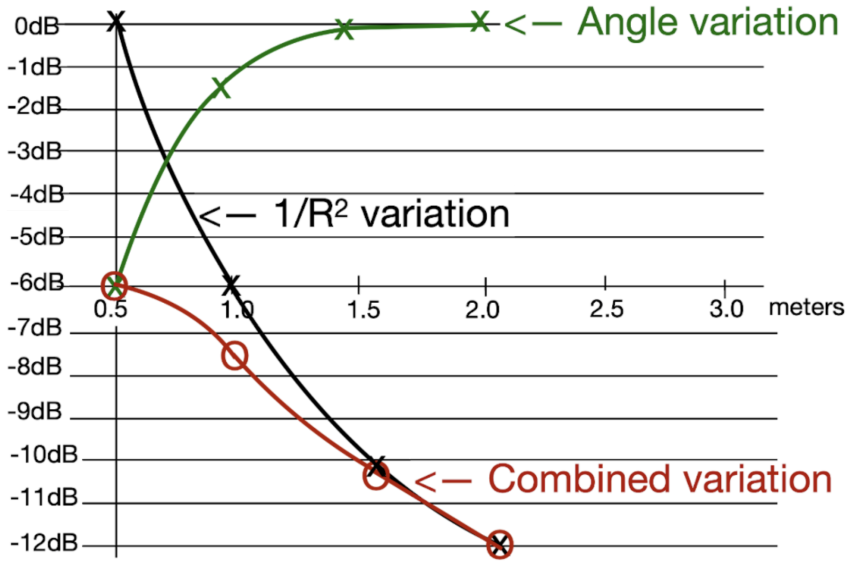
This figure demonstrates our testing (red) in comparison to the ISL (green).

The figure below depicts the area that our antenna will cover. It is set from a top-down view of the antenna, with the left side depicting the reflector elements, and the right side depicting the signal that is going through the director elements. We can infer that the signal is not only affected by things in front of the antenna, but also by elements behind it, which helps us filter out unnecessary data that we receive.

Figure VII: Yagi-Antenna covers

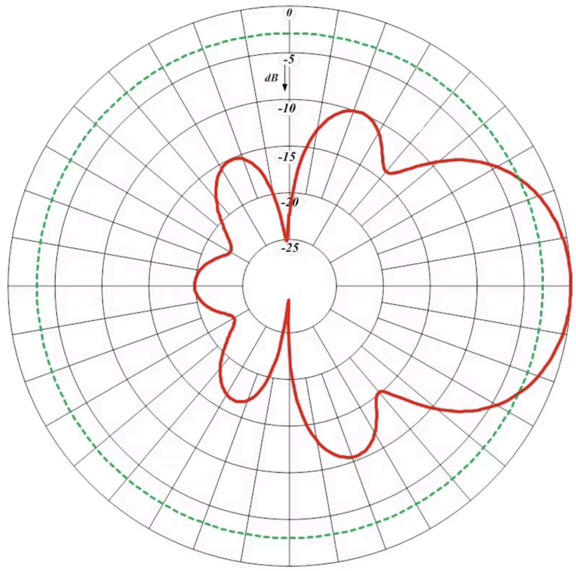

This figure shows a polar representation of the antenna’s signal gain.

Analysis code

The code for this project aimed to plot the difference in amplitude of the VNA transmission coefficient (S21) relative to a calibration. This code will first initialize the necessary libraries used for communication, then require the user to create a calibration measurement, wherein the system will be cleared of any objects in its surrounding fields. This calibration can be overwritten as the unit moves around an area. After the calibration, the code will enter an infinite loop where it will start plotting out the difference in amplitude between the calibrated S21 and the most recent S21 measurement. This will also plot out the most recent S21 measurement with respect to its difference (display), its amplitude calibration, and its recent S21 amplitude. From these curves, we will extract a feature set, which will then be used in later machine learning for further analysis.

Block I: VNA & Plot Initialization

```
# Import the necessary libraries
import pynanovna, math, keyboard
import numpy as np
import matplotlib.pyplot as plt

# Initialize the VNA serial link
vna = pynanovna.VNA()

#Sets frequency range and number of points to sweep
vna.set_sweep(850, 900, 101)

# set the dB calibration to -∞
dBCalibrate = -math.inf

# create blank arrays to differentiate the complex64 int parts
real = []
imaginary = []

# initialize VNA data stream and add condition to start
# data analysis
stream = vna.stream()
hasCalibd = False

# enable interactive plot
plt.ion()

# for all collected parameters in the VNA stream
for s11, s21, frequencies in stream:
    <Continued in Block II & III>
```

Block II: Local Calibration

```
# if the C key on the keyboard is pressed, init calibration
if keyboard.is_pressed('c'):
    # extract real and imaginary number parts
    real = np.real(s21)
    imaginary = np.imag(s21)

    # this is the equivalent of |S21| = sqrt(Re{S21}^2 + Im{S21}^2)
    dBCalibrate = np.sqrt(np.add(np.square(real), np.square(imaginary)))
    hasCalibd = True
```

Block III: Data analysis, saving, and plotting

```
# once an initial calibration has been taken,
# start plotting data asap
if hasCalibd:
    # extract real and imaginary number parts
    realAfterCalib = np.real(s21)
    imaginaryAfterCalib = np.imag(s21)

    # equivalent of |S21| = sqrt(Re{S21}^2 + Im{S21}^2)
    dBMeasure = np.sqrt(np.add(np.square(realAfterCalib), np.square(imaginaryAfterCalib)))
    dBDisplay = dBMeasure - dBCalibrate

    # this is a measure of the average amplitude (of magnitude)
    # over the dbDisplay time.
    RMSDisplay = np.sqrt(np.sum(np.square(dBDisplay)))

    # initializes plot
    plt.clf()
    plt.figure(figsize=(10, 6))

    # plots out the magnitude, raw frequency, and s21 relative to different frequencies.
    plt.plot(dBDisplay/850, 'r', label='|s21| magnitude')
    plt.plot(frequencies/850, 'b-', label='measured s21 (raw freq)')
    plt.plot(frequencies/850, dBDisplay, 'g-', label='measured s21 rel. to display')
    plt.plot(frequencies/850, dBCalibrate, 'y-', label='measured s21 rel. to calibrate')
    plt.plot(frequencies/850, dBMeasure, 'm-', label='measured s21 rel. to last measure')
    plt.xlabel("Frequency (MHz)")
    plt.ylabel("Magnitude (dB)")
    plt.title("Average magnitude (dB): " RMSDisplay)

    # draws the plot
    plt.draw()
    plt.pause(0.01)
```

Results

We conducted a number of tests throughout our project's development, and these results proved to be indicative of the ability of detecting people using signal interference. This was a preliminary study without the use of snow or alternatives, as our prototype still had small issues. These tests included different environments, different antennas, and different angles, wherein Figure IX and X demonstrate the biggest difference with signal strength at different distances. Our tests involved the use of a team member, however, there was no additional risk other than that of daily life. The data below demonstrates the antenna's signal strength across the range of 850-900MHz, and first starts off with no subject interference. This subject is then placed 1ft, 5ft, 10ft, and 15ft away from the antenna.

Figure VIII: S21 Test I

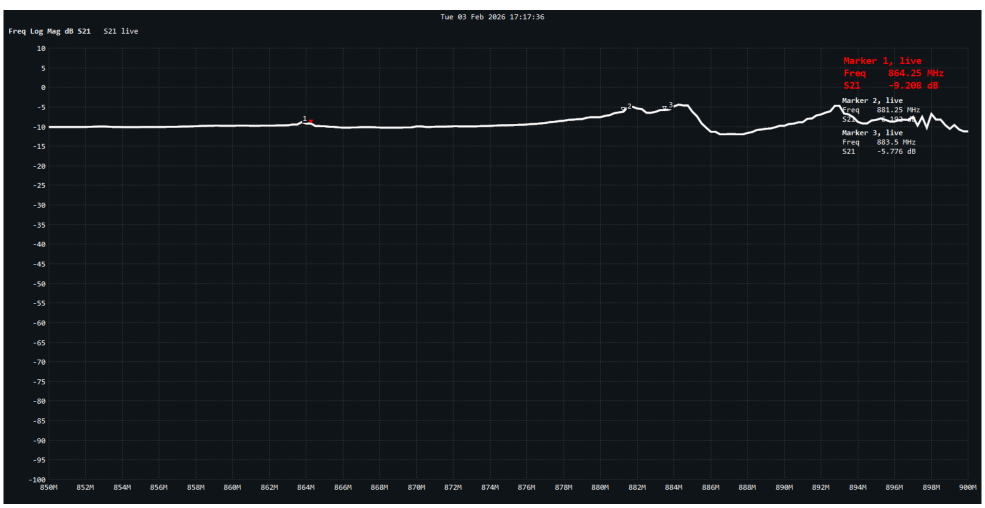

Data with no person in sight. S21 gain loss: -9.208 dB

Figure IX: S21 Test II
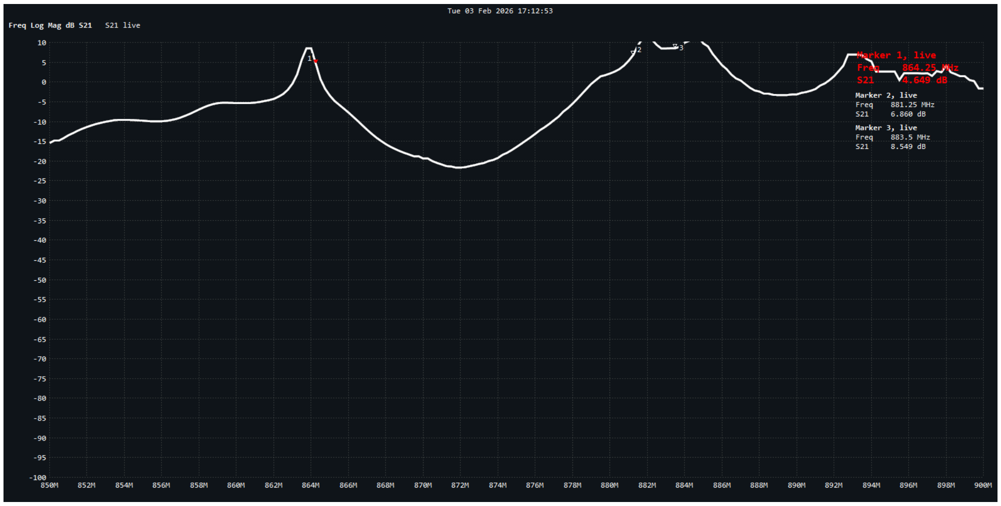
Data with a person 1ft away. S21 gain loss: 4.649 dB

Figure X: S21 Test III
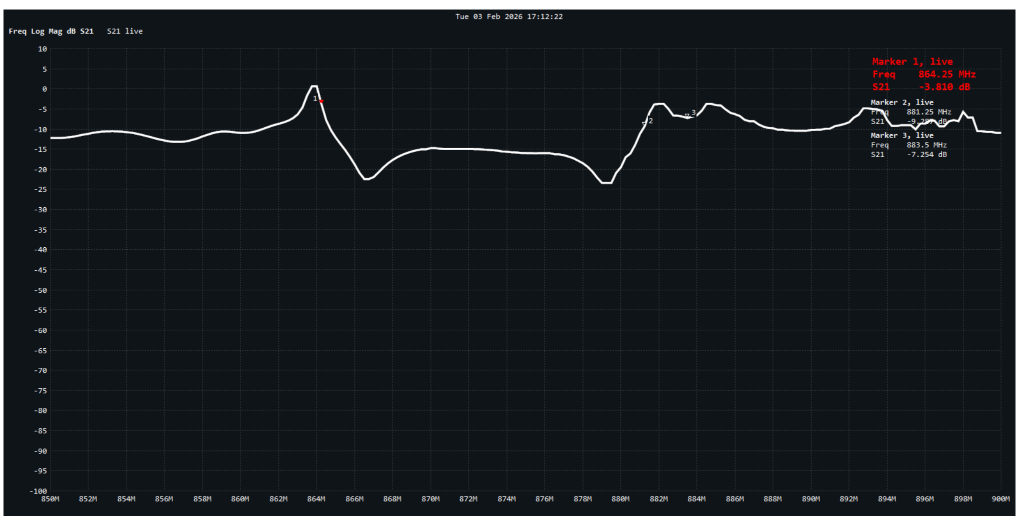
Data with a person 5ft away. S21 gain loss: -3.810 dB

Figure XI: S21 Test IV

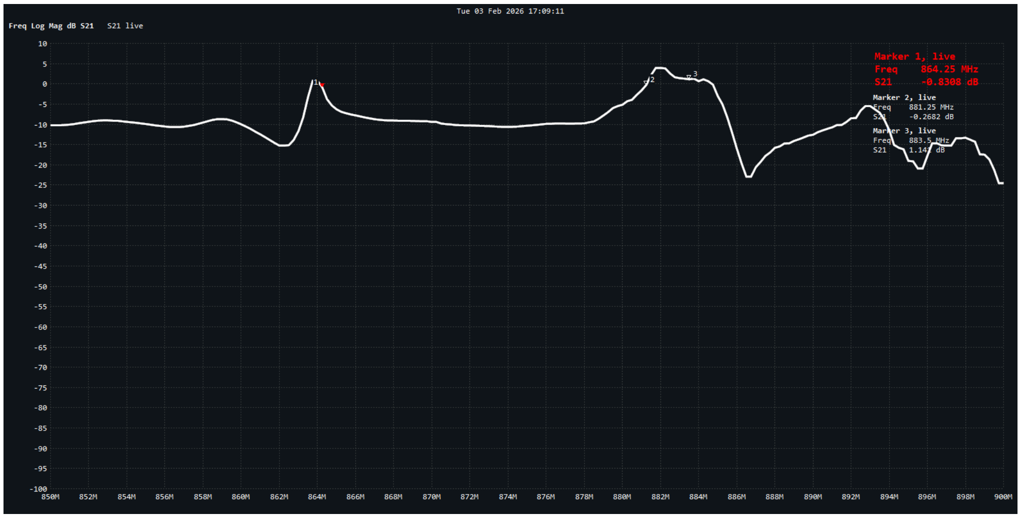

Data with a person 10ft away. S21 gain loss: -0.8308 dB

Figure XII: S21 Test V

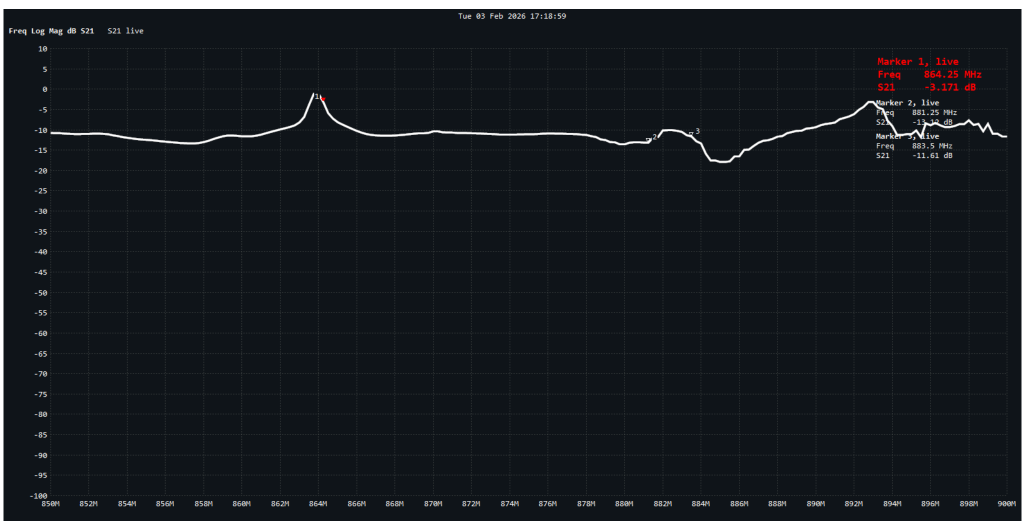

Data with a person 15ft away. S21 gain loss: -3.171 dB

Discussion

These results demonstrated that our antennas did have the capabilities of detecting people. However, they were problematic due to cross talk discrepancies, and small design variations in our system. Furthermore, the code analysis had trouble with data parsing, and the usage of real/imaginary numbers, as NumPy, the library that handles complex number forms, had a hard time parsing and extracting the real and imaginary number parts, which could have led to issues with our 2D array operations.

Conclusion

This system is a work in progress and will require more research and development to further refine, with many future plans for improvement being outlined in the section below. The tests that we have conducted indicate that the detection of individuals is possible, but design variations, such as antenna distance, shield size, and other small discrepancies cause unwanted issues.

Future plans

Future plans for this project include mitigating the amount of cross talk that occurs between the antennas, conducting further research and tests using snow alternatives, and further refining the analysis code for implicit detection of individuals. Many of these goals will require the reconstruction of the project and addition of elements, such as filters for data (Savitszky-Golay), use of Machine Learning for classification, and the optimization of antennas.

Acknowledgements

We would like to express our unwavering gratitude to our mentor, Dave Ritter, for his invaluable guidance, support, and patience throughout our project. His feedback and suggestions for our project helped shape the methodology greatly. We would also like to thank our teacher sponsor, Irina Cislaru, and furthermore, guiding teacher, Barbara Teterycz, for supporting our project during school hours and connecting us with our current team members. Finally, we would like to thank MAKE Santa Fe for allowing us to use their workspace, tools, and support to help us assemble our project. We gratefully acknowledge and thank everyone who contributed to this project.

References

Avalanche problems. (n.d.). Bridgeport Avalanche Center. https://bridgeportavalanchecentwer.org/avalanche-problems/

Delgadillo, M., & Maringan P. (2009). 2.4 GHz Yagi-Uda Antenna. [PowerPoint presentation]. San José State University. EE 172. https://www.sjsu.edu/people/raymond.kwok/docs/project172/Yagi_antenna_2r4G_2009.pdf

Dukowitz, Z. (2025, May 6). Ground penetrating radar (GPR): An in-depth guide. MFE Inspection Solutions. https://mfe-is.com/ground-penetrating-radar/

Ferrara, V., & Chizh, M. (2017). Action TU1208 Civil Engineering Applications of Ground Penetrating Radar Guide to building a GPR radar for educational use Sections: RF Hardware design, Firmware of microcontroller, and management software. National Institute of Telecommunications of Poland.

https://gpradar.eu/onewebmedia/TU1208_GPRforeducationaluse_November2017_FerraraChizhPietrelli.pdf

Genswein, M., Atkins, D., Obad, J., Grady, E., Piché, M., Guyn, T., Whelan. R., Brattlien, K. (n.d.). Recommendation on How Avoid Interference Issues in Companion and Organized Avalanche Rescue. https://arc.lib.montana.edu/snow-science/objects/ISSW13_paper_P1-34.pdf

Grasegger, K., Strapazzon, G., Procter, E., Brugger, H., & Soteras, I. (2016). Avalanche Survival After Rescue With the RECCO Rescue System: A Case Report. Wilderness & environmental medicine, 27(2), pp. 282–286. https://doi.org/10.1016/j.wem.2016.02.004

McIntosh, S. E., Grissom, C. K., Olivares, C. R., Kim, H. S., & Tremper, B. (2007). Cause of death in avalanche fatalities. Wilderness & environmental medicine, 18(4), pp. 293–297. https://doi.org/10.1580/07-WEME-OR-092R1.1

Talbot-Smith, M. (1993). 8 - Sound, speech and hearing. In F. Mazda (Ed.), Telecommunications Engineer’s Reference Book (pp. 8-1-8–16). doi:10.1016/B978-0-7506-1162-6.50014-9

Avalanche Safety. (n.d.). US Department of Commerce, NOAA, National Weather Service. www.weather.gov/safety/winter-avalanche

Wikipedia contributors. (2026, February 22). List of avalanches by death toll. Wikipedia, The Free Encyclopedia. https://en.wikipedia.org/w/index.php?title=List_of_avalanches_by_death_toll&oldid=1339769354

Wikipedia contributors. (2026, February 27). Yagi–Uda antenna. In Wikipedia, The Free Encyclopedia. https://en.wikipedia.org/w/index.php?title=Yagi%E2%80%93Uda_antenna&oldid=1340802434

Zhang, M., Wang, Y., Hu, Q., Zhao, S., Liang, L., Chen, Y., Lei, Y., Qiu, C., Jia, P., Song, Y., Qin, L., & Wang, L. (2023). Phase-Modulated Continuous-Wave Coherent Ranging Method and Anti-Interference Evaluation. Applied Sciences, 13(9), 5356. https://doi.org/10.3390/app13095356